

A Three-Stage Classifier for Remote Sensing of Mountain Environments

Steven E. Franklin and Bradley A. Wilson*

Department of Geography, The University of Calgary, Calgary, Alberta T2N 1N4, Canada

ABSTRACT: The use of spatial satellite image information and digital elevation models in remote sensing classification is described for a mountainous region in southwest Yukon. A three-stage classification method was devised that incorporates a quadtree-based segmentation operator, a Gaussian minimum-distance-to-means test, and a final test involving ancillary geomorphometric data and a spectral curve measure. The overall increase in accuracy is significant compared to maximum-likelihood techniques, and the resulting map products are consistent with few unclassified areas. The three-stage classifier can produce an output map in significantly less time than that required for the per-pixel maximum-likelihood classifier, and used a minimum of field or training data which are often difficult and expensive to acquire in complex terrain. The programs to handle geomorphometric, spatial and spectral attributes are coded efficiently in the C programming language. They can be adapted to find homogeneous regions in high resolution aerial imaging spectrometer data sets (sub-metre pixel resolution) or other raster databases.

INTRODUCTION

SATELLITE REMOTE SENSING IMAGE CLASSIFICATION ACCURACIES in complex terrain can be increased by using information from ancillary sources (Strahler, 1981; Hutchinson, 1982; Frank, 1988; Jones *et al.*, 1988) and image spatial characteristics (Snyder and Cowart, 1983; Tannous and Arif, 1989; Tailor *et al.*, 1986; Peddle and Franklin, 1991). The classification may be accomplished using an augmented set of variables that includes (for example) geomorphometry and estimates of neighborhood variability such as entropy derived from spatial co-occurrence. Image spatial characteristics also have been used in segmentation schemes and compared to results obtained using only per-pixel information. Cross *et al.* (1988) discussed pre-processing and post-processing spatial techniques, and summarized some earlier attempts to drive image segmentation with spatial information such as the ECHO system (Kettig and Landgrebe, 1976; Landgrebe, 1980). The pre-processing techniques are designed to reduce the number of computations required and to make decisions on class membership as early as possible in the classification. At the heart of these classifiers is the search for edges and homogeneous regions (e.g., Haralick, 1980; Pavlidis, 1982; Tilton and Cox, 1983; Qui and Goldberg, 1985; Bousquet and Flouzat, 1986) and the orderly division or aggregation of pixels using data structures (e.g., Spann and Wilson, 1985; Paine, 1987). An underlying theme in these developments has been the recognition that different approaches to classification may be needed for different parts of the image.

The pixels within a satellite image contain a high degree of spatial correlation, but per-pixel classifiers ignore this intuitive relationship and decide class membership based on single pixel spectral response patterns alone (Khazenie and Crawford, 1990). Spatial classifiers attempt to quantify the degree of spatial correlation and use this information together with the spectral response pattern to decide class membership. Because all natural scenes, and all raster data sets, contain a certain degree of this spatial coherence, classifiers that take note of some measure of spatial homogeneity can yield higher classification accuracy. In this paper, a three-stage classifier is introduced with an example multispectral satellite classification of landcover in the mountainous southwest Yukon (Figure 1). The classification proceeds with (1) a quadtree-based segmentation and test for homoge-

neous regions, (2) a normal per-pixel classification test, and (3) a test involving ancillary digital elevation data and a spectral curve measure. One important feature of this three-stage approach is that unnecessary calculations are reduced; as soon as a pixel or region passes one of the tests at an early stage, no further work at that location is required. The procedure is an efficient way of incorporating ancillary data into one or more of the stages. For example, one useful ancillary source of information in a mountain environment is a digital elevation model which provides highly diagnostic variables such as slope and aspect angle. This information is not always required to make correct decisions on landcover, however, and therefore the inclusion of these variables in all decisions made for every pixel ensures a large degree of inefficiency. The three-stage classifier



FIG. 1. Physiographic features of the study area in Kluane National Park, southwest Yukon.

* Presently with INTERA Technologies Ltd., 2500-101 6th Avenue S. W., Calgary, Alberta T2P 3P4, Canada.

attempts to classify pixels with the minimum information; only when no decision can be made will the ancillary data be consulted. The procedure has been designed to avoid some of the notable problems with classifiers that rely solely on parametric statistics, such as the increasing sensitivity to increasing numbers of mapping variables (Tom and Miller, 1984; Kenk *et al.*, 1988; Lee and Landgrebe, 1990; Franklin and Wilson, 1991a). In the coming *hyperspectral* era of remote sensing, single pass per-pixel classifiers will not be adequate for many classificatory tasks.

A THREE-STAGE CLASSIFICATION ALGORITHM

The classifier described here is based on three stages of operation: (1) a quadtree segmentation and test for homogeneity, (2) a minimum distance to means test, and (3) a spectral curve and geomorphometric data test. The programs (described in detail in Franklin and Wilson, 1991b) accept any square raster data input with dimensions of 512 pixels by 512 lines that can be divided into four equal square quadrants recursively until the one pixel level is reached.

STAGE ONE CLASSIFIER—QUADTREE SEGMENTATION AND HOMOGENEITY

One method of segmentation that does not require knowledge of the characteristics of the data is the quadtree approach (Pavlidis, 1982; Spann and Wilson, 1985). This approach assumes that spatial coherence exists, but makes no assumption about the area over which spatial characteristics are to be measured. Any image can be subdivided into four equal partners, or quads, successively until the one pixel level is reached. Each quad is tested for homogeneity after successive partitioning. If the quad passes the test, an attempt to classify the entire quad can be made. If classification is successful, no further work is required. If classification fails, the quad is divided further into four equal areas and the test for homogeneity is repeated on each partner. Quadrees can begin with the entire scene as the first block to be tested and partitioned (top-down), or with single pixels that are merged into quad regions successively. This latter technique has been termed the split-and-merge process (Spann and Wilson, 1985; Cross *et al.*, 1988).

The quadtree method is data independent because it does not evaluate the data in any manner during segmentation. This independence has several advantages beginning with the recursive nature of the algorithm. Programming is simplified (see Franklin and Wilson, 1991b) and efficient. No arbitrary decisions are made concerning the location of boundaries between different homogeneous regions. The quadtree examines whether or not a quad is homogeneous, not whether it falls inside a homogenous region or has an edge or class boundary pass through. The final decision to be made can conform to standard classification or clustering decision rules. Therefore, the first-stage segmentation of the image data is unsupervised and knowledge about the classes or distribution of features in the image is not required at this point (Cross *et al.*, 1988). The segmentation is performed by a procedure that calls itself four times, passing two new parameters that include the starting point (top left corner of the quad) and the dimension of the quadtree. The first level of segmentation is taken to size 32 by 32 to reduce the many calculations at large quad sizes that would most likely fail the test for homogeneity. The final level of segmentation is size 4 by 4; areas smaller than this yield unstable statistics for test purposes.

The homogeneity test employed uses the coefficient of variance (Tannous and Arif, 1989) and range statistics (Cross *et al.*, 1988) for each input spectral band. These statistics were selected because of their simplicity and the need to optimize the execution speed of the algorithm for the small microcomputers (Compaq 386/25 DESKPRO; AST Research 386/20 Premium)

available for this research; obviously, more complex tests could be used in their place. A threshold value of 14 percent was selected for the coefficient of variance after extensive testing of several satellite images. For example, if the threshold was lowered, an unacceptably large number of quads failed the test. The algorithm calculates a coefficient of variance for each segmented quad of pixels. If a quadrant has a lower coefficient of variance than the threshold value, it is homogenous. A special case occurs when the quadrant mean value is very low (approximately less than five) and the coefficient of variance is not stable. In that case, the range of pixel values is calculated and compared to a homogeneous range of three. The program can be terminated at this point. Alternatively, an attempt can be made to label the homogeneous regions and to deal with areas that have failed the homogeneity test.

When a homogeneous quadrant is discovered, the mean and variance are compared to the mean and variance of known classes in the region sampled with training data. The known class statistics are stored in the form of a "seed file" and may have been acquired through field sampling, a previous classification, a spectral library, or initial clustering procedures. The first test is a variance test based on the F-statistic. The second test is a Student's t-test which compares means of the sample (the homogeneous quadrant) and the population (the training data for each class). If no significant differences are found, each pixel in the quadrant is assigned to that particular class and eliminated from further processing. If several classes pass the test, the quadrant is assigned to the class with the lowest cumulative t-test value in all the available bands.

STAGE TWO CLASSIFIER—MINIMUM DISTANCE TO MEANS

Stage two of the classifier is a straightforward minimum-distance-to-means calculation with stringent acceptance criteria. Pixels that have not been identified during the quadtree segmentation may be handled best in a per-pixel decision rule without reference to spatial characteristics. For simplicity and ease of use, we have selected the minimum-distance-to-means classifier based on standard deviation distances. Jensen (1986) has suggested that this formulation can give comparable results to more sophisticated decision rules such as maximum-likelihood, particularly if the classes are "distinct." Problems with data set dimensionality (Swain and Davis, 1978; Tom and Miller, 1984) and modifying thresholds (Kenk *et al.*, 1988) can be avoided.

The distances between each pixel value and each known class mean are computed by subtracting these two values and dividing by the class standard deviation. Because each pixel is compared to each class once, a method of eliminating highly unlikely assignments as soon as possible was implemented by thresholding incoming values at two standard deviations.

STAGE THREE CLASSIFIER—ANCILLARY DATA AND SPECTRAL CURVES

Some pixels in a given image will not be correctly identified in either stage one (quadtree segmentation) or stage two (minimum-distance-to-means). In our remote sensing research in mountain areas, these problem pixels require a third stage that employs an entirely different set of tests and involves the use of ancillary information independent of the satellite image data. For example, many of these problem pixels fall in areas of mountain shadows; they are spectrally variable because they contain diffuse radiation and backscattered light, and they do not resemble classes sampled in the conventional way (means and variances). We can resolve these classification problems with recourse to an ancillary elevation model data set, and by examining spectral curves. In other images, pixels that remain unclassified after the first two passes may be transitional between regions or boundaries between classes, or they may con-

tain significant noise, artifacts (such as clouds), or an unknown feature. Other formulations for the third stage in the classifier may be appropriate for these pixels.

The elevation model information can be examined for homogeneity and similarity to the existing geomorphometric conditions in the known classes. This is a repetition of the first two stages using geomorphometric variables rather than spectral variables. The spectral data are retained and compared to the known classes in the form of a spectral curve (Carlotto, 1986). This curve is a graphical representation of the mean values for the known classes; the idea is to compare the incoming pixels' curve to the known classes to determine whether the relationship between the bands is consistent with a known class. For example, if a class has mean spectral response values in four bands equal to 10, 20, 15, 50, the curve would be described as up (10 > 20), down (20 > 15), up (15 < 50). Carlotto (1986) demonstrated that some pixels affected by shadows or atmospheric attenuation exhibited much lower pixel values but had a similar spectral curve to those fully illuminated pixels sampled in a class. A shadowed pixel of surface material from that class would have the same curve for those four bands: up, down, up. Again, in our software, the ancillary geomorphometric variables are checked for similar relationships; this substantially reduces the number of classes with similarly shaped curves.

THE EXPERIMENT

STUDY AREA AND DATA COLLECTION

A study area in Kluane National Park, southwest Yukon, was selected for a test of the three-stage classifier and a comparison to the maximum-likelihood decision rule. This area is mountainous with extreme local environmental gradients characteristic of a high arctic, paraglacial terrain. A SPOT MLA satellite image was acquired on 29 July 1989 with a viewing angle of +17.22 degrees west, and solar illumination conditions of 47.76 degrees elevation, 174.63 degrees azimuth. The image was cloudfree and without visible radiometric degradation; however, no adjustments were made for atmospheric influences or the effect of the wide-angle viewing geometry. An elevation model was generated by manually digitizing a 1:50,000-scale contour map and interpolating a dense grid with the Surface II Graphics System (Davis, 1987). The DEM and satellite imagery were co-registered using 20 ground control points. A 0.5-pixel error was tolerated during the DEM resampling; geomorphometric measures of elevation, slope angle, and incidence value were computed. The preparation of the data is described in some detail in Franklin and Wilson (1991a).

Field data on percent vegetation cover and species and topographic conditions were collected at 793 randomly selected sites corresponding to 11 landcover classes. These data were used in two ways: (1) as core sites for training the maximum-likelihood algorithm and as input to the three-stage classifier, and (2) as test sites to determine classification accuracy after mapping. Because the pixels selected for field visits were used in both defining decision rules and in verifying their accuracy, the absolute mapping accuracies are known to be overestimated.

Two methods of classification were used to map the area in the satellite image. The first was a straightforward application of the supervised maximum-likelihood classifier available in the PCI Inc. (1988) EASI/PACE image analysis system. Thresholds were not modified to account for class overlap (Kenk *et al.*, 1988); this action serves only to increase commission errors with other classes rather than the null class. The second method was a thorough test of the three-stage classifier. Both classifiers were run on a 20MHz IBM-AT clone under MS-DOS with six data channels (three multispectral, three topographic) and 11 classes.

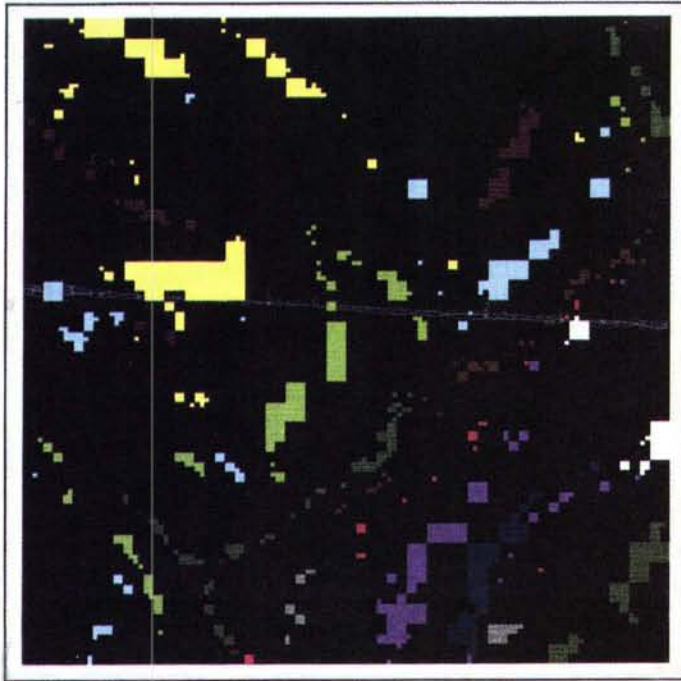
RESULTS OF CLASSIFICATION

An execution time of approximately 45 minutes was recorded for the new, three-stage algorithm. The same classification based on maximum-likelihood decision rules required approximately 60 minutes. The main differences recorded in these two tasks were the number of pixels classified (92 percent versus 61 percent), and the overall accuracies achieved (87 percent versus 56 percent). Table 1 provides a summary of the individual class accuracies and overall performance for the two methods. It is important to note that, in order to avoid ill-conditioned covariance matrices for individual classes, the maximum-likelihood classifier required data input of over 42,000 pixels obtained by interactively training on each class. The three-stage classifier required a seed file of means and standard deviations constructed from the 793-pixel field sites.

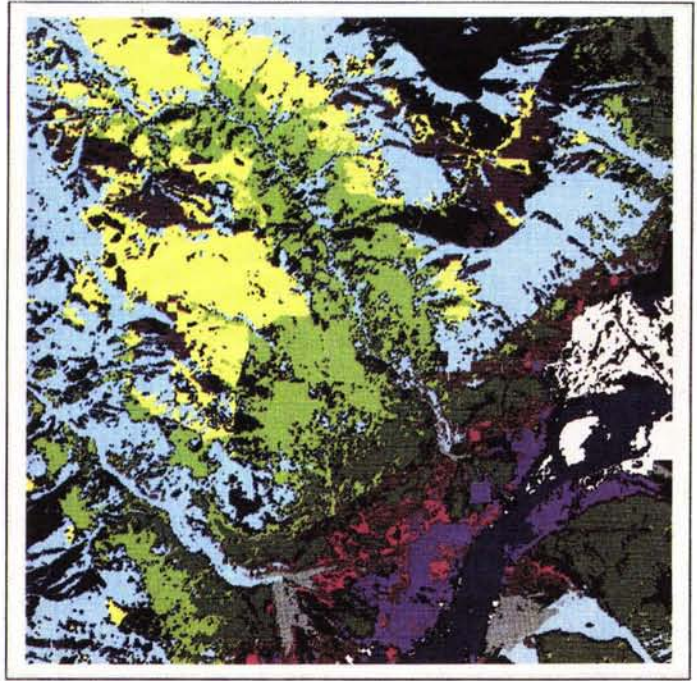
The maximum-likelihood classifier yielded 71.86 percent accuracy overall using the three SPOT bands. This decreased to 67.34 percent with the addition of elevation to the decision rule, 60.36 percent with elevation and incidence value, and 55.98 percent with elevation, incidence, and slope. The table also shows the percent accuracy of only those pixels classified in each attempt. The decrease in accuracy can be seen to be a direct function of the increasing numbers of unclassified pixels, and may be indirectly related to their statistical properties. For example, elevation model data often do not conform to the multivariate normal distribution; nor are the individual variables indepen-

TABLE 1. SUMMARY OF MAXIMUM-LIKELIHOOD AND THREE-STAGE TOPOGRAPHIC CLASSIFICATIONS (793 TEST PIXELS)

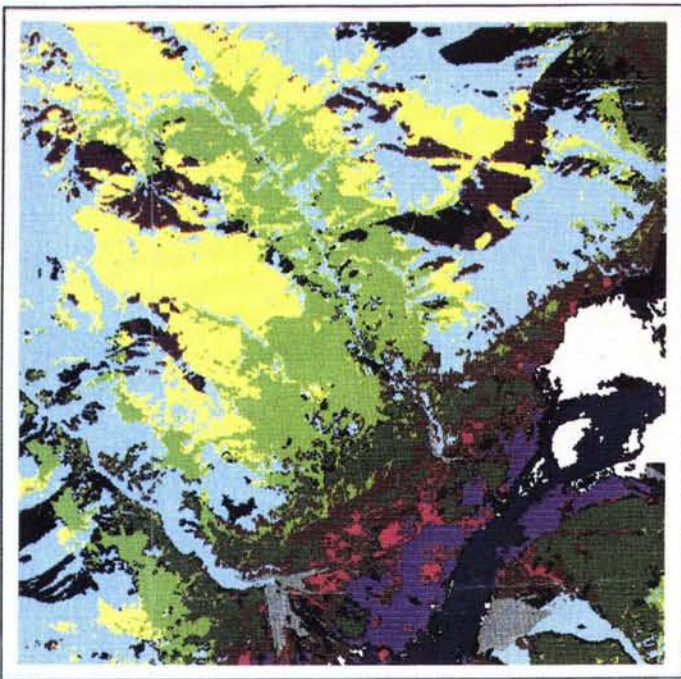
Class	(MLC) SPOT-MLA alone		(MLC) SPOT-MLA + Elevation		(MLC) SPOT-MLA + Elevation + Incidence		(MLC) SPOT-MLA + Elevation + Incidence + Slope		(Topographic) SPOT-MLA + Elevation + Incidence + Slope	
	Overall%	Classed%	Overall%	Classed%	Overall%	Classed%	Overall%	Classed%	Overall%	Classed%
Coniferous	67.00	68.57	62.04	89.33	52.78	86.36	48.15	88.14	98.15	98.15
Deciduous	42.70	44.71	7.08	82.50	23.60	77.78	23.60	77.78	70.79	70.79
Mixed	88.89	88.89	86.11	96.88	75.00	87.10	66.67	96.00	44.44	44.44
Organic	88.89	88.89	88.89	90.00	81.48	89.19	77.78	91.30	98.77	100.00
Alpine Tundra	71.25	71.25	71.25	78.08	70.00	98.25	56.25	100.00	91.25	91.25
Alpine Meadow	57.95	61.45	37.50	55.93	27.27	57.14	20.45	64.29	93.18	93.18
Barrens	74.44	81.71	78.89	98.61	75.56	100.00	74.44	100.00	100.00	100.00
Alluvial Dep.	95.65	95.65	95.65	100.00	89.86	100.00	81.16	100.00	100.00	100.00
Water	75.00	75.00	75.00	79.41	75.00	79.41	75.00	79.41	94.44	94.44
Delta	68.57	75.00	42.86	78.95	42.86	78.95	42.86	78.95	100.00	100.00
Montane Grass.	60.49	63.64	65.43	91.38	50.62	89.13	49.38	90.91	69.14	78.87
Averages	71.86	74.07	67.34	85.55	60.36	85.76	55.98	87.89	87.29	88.28



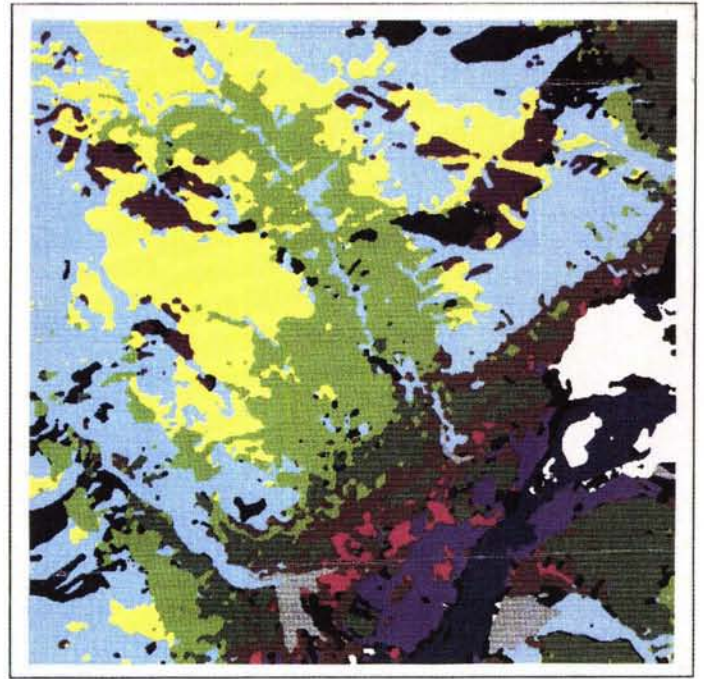
(a)



(b)



(c)



(d)

Legend











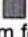
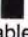
	1. Coniferous Forest		5. Alpine Tundra		9. Water
	2. Deciduous Shrub		6. Alpine Meadow		10. Delta
	3. Mixed Forest		7. Barrens		11. Montane Grassland
	4. Organic Terrain		8. Alluvial Deposits		12. Unclassified

PLATE 1. Map output of the three-stage classification algorithm for classes listed in Table 1. (a) First-stage quadtree segmentation and homogeneity test; approximately 14 percent of the image has been classified. (b) Second-stage minimum-distance-to-means test; approximately 76 percent of the image has been classified. (c) Third-stage topographic test and spectral curve measures; approximately 92 percent of the image has been classified. (d) Postclassification smoothing of noise and unclassified areas; final map accuracy is determined to be 87.64 percent correct compared to field identification of 793 pixels.

dent. These results are consistent with accuracies obtained by other researchers in similar experiments (Kenk *et al.*, 1988; Jones *et al.*, 1988). The final columns in Table 1 show the results after the three-stage classification. Overall accuracy is 87.29 percent with less than 9 percent remaining unclassified. The comparison to maximum-likelihood highlights the important fact that almost 30 percent more of the image has been classified with very high accuracy.

The maps in Plate 1 illustrate the progress of the three-stage algorithm: (a) first-stage classification of 14 percent of the image at 89.01 percent accuracy; (b) second-stage classification of 62 percent of the image at 91.32 percent accuracy; and (c) third-stage classification of 15 percent of the image at 87.02 percent accuracy. Approximately 8 percent of the image remained unclassified. These are pixels in the deepest shadows or are "mixed-pixels" (mixels) for which no decision can be made without high probability of error. The final image in Plate 1 was obtained after postclassification smoothing or reclassification of pixels based on majority membership in a 3 by 3 window (Thomas, 1980; Booth *et al.*, 1989). Accuracy of this product based on the 793 field sites is 87.64 percent with a confidence interval of 85.90 to 92.65 percent.

CONCLUSION

A new, three-stage classifier has been developed to handle high spatial and spectral resolution remote sensing data and to permit efficient incorporation of ancillary data variables in the analysis. The basic ideas are to classify certain parts of an input image with the spatial or spectral characteristics most suitable for decision making and to avoid formulations that display sensitivity to increasing numbers of mapping variables and their statistical properties. Pixels are classified at the earliest stage possible to reduce unnecessary work, and training the classifier has been reduced to a minimum. The first stage is a quadtree segmentation and homogeneity test that uses the coefficient of variance and range statistics. Approximately 14 percent of the Yukon SPOT MLA image was classified after this process. The second stage is a Gaussian minimum-distance-to-means classifier with F-statistics and Student's t-test. A total of 76 percent of the satellite image was classified after these two passes were complete. The third stage of the classification algorithm employs geomorphometric ancillary data and spectral curves to decide pixel identity. This procedure classified approximately 15 percent of the entire scene, leaving less than 9 percent unclassified.

The overall accuracy of the final map (which was later smoothed) reached 87.64 percent. This compares favorably with the 71.86 percent achieved with SPOT MLA data alone and the 55.98 percent achieved with the SPOT MLA data plus elevation, slope, and incidence value from the digital elevation model in the maximum-likelihood formulations. When the unclassified pixels are not used in the calculation of maximum-likelihood accuracy, the final numbers are more comparable; however, the new classifier made correct decisions on 30 percent more pixels than the maximum-likelihood classifier. The three-stage classifier can produce an output map in significantly less time than that required for the per-pixel classifier, and used a minimum of field or training data which are often difficult and expensive to acquire in complex terrain. The programs to handle spatial and spectral attributes are coded efficiently in the C programming language (see Franklin and Wilson, 1991b). They can be adapted to segment and classify homogeneous regions in high resolution aerial imaging spectrometer data sets (down to sub-metre pixel resolution) or other raster databases. The spatial classification techniques discussed here will be increasingly important in the coming *hyperspectral* era of remote sensing.

ACKNOWLEDGMENTS

This research was funded by the Natural Sciences and Engineering Research Council of Canada and Parks Canada Contract No. K3509-CR-88-21. Additional support was obtained through the Arctic Institute of North America, Department of Indian and Northern Affairs, Alberta STEP Grants and The University of Calgary. The assistance of Mr Doug Fortune in the programming effort is gratefully acknowledged. SPOT satellite imagery are copyright, CNES 1989.

REFERENCES

- Booth, D. J., T. R. Chidley, and W. G. Collins, 1989. Integration of context classifiers with GIS, *Proc. International Geoscience and Remote Sensing Symposium*, Vancouver, B.C., pp. 656-659.
- Bousquet, P., and G. Flouzat, 1986. Segmentation by mathematical morphology processing on the image understanding model in remote sensing, *Proc. International Geoscience and Remote Sensing Symposium*, Zurich, Switzerland, pp. 553-557.
- Carlotto, M. J., 1986. Extracting surface features in multispectral imagery, *Proc. International Geoscience and Remote Sensing Symposium*, Zurich, Switzerland, pp. 283-288.
- Cross, A. M., D. C. Mason, and S. J. Dury, 1988. Segmentation of remotely sensed images by a split-and-merge process: *Intern. Jour. Remote Sensing*, Vol. 9, No. 8, pp. 1329-1345.
- Davis, J. C., 1987. Contour mapping and Surface II: Science, Vol. 237, No. 4815, pp. 669-677.
- Franklin, S. E., and J. E. Moulton, 1990. Variability and classification of Landsat Thematic Mapper spectral response in southwest Yukon: *Canadian Jour. Remote Sensing*, Vol. 16, No. 1, pp. 2-13.
- Franklin, S. E., and B. A. Wilson, 1991a. Vegetation mapping and change detection using SPOT MLA and Landsat TM data in Klane National Park: *Canadian Jour. Remote Sensing*, Vol. 17, No. 1, pp. 2-17.
- , 1991b. Spatial and spectral classification methods in remote sensing: *Computers & Geosciences* (in review).
- Haralick, R., 1980. Edge and region analysis of digital image data: *Computer Graphics and Image Processing*, Vol. 6, No. 3, pp. 456-465.
- Hutchinson, C. F., 1982. Techniques for combining Landsat and ancillary data for digital classification improvement: *Photogrammetric Engineering & Remote Sensing*, Vol. 48, No. 1, pp. 123-130.
- Jensen, J. R., 1986. *Introductory Digital Image Processing, A Remote Sensing Perspective*: Prentice-Hall, Englewood Cliffs, New Jersey, 379p.
- Jones, A. R., J. J. Settle, and B. K. Wyatt, 1988. Use of digital terrain data in the interpretation of SPOT-1 HRV multispectral imagery: *Intern. Jour. Remote Sensing*, Vol. 9, No. 4, pp. 669-682.
- Kettig, R. L., and D. A. Landgrebe, 1976. Classification of multispectral image data by extraction and classification of homogeneous objects: *IEEE Transactions on Geoscience Electronics*, Vol. 14, No. 1, pp. 19-26.
- Kenk, E., M. Sondheim, and B. Yee, 1988. Methods for improving the accuracy of Thematic Mapper ground cover classifications: *Canadian Jour. Remote Sensing*, Vol. 14, No. 1, pp. 17-31.
- Khazenie, N., and Crawford, M., 1990. Spatial-temporal autocorrelated model for contextual classification: *IEEE Transactions on Geoscience and Remote Sensing*, Vol. 28, No. 4, pp. 529-539.
- Landgrebe, D. A., 1980. The development of a spectral-spatial classifier for earth observational data: *Pattern Recognition*, Vol. 12, No. 2, pp. 165-175.
- Lee, C., and D. A. Landgrebe, 1990. Fast multistage Gaussian maximum likelihood classifier: *Proceedings, International Geoscience and Remote Sensing Symposium*, College Park, Maryland, pp. 349-352.
- Paine, S., 1987. *Information Extraction from Digital Landsat Imagery for Integration into an LRS*: unpubl. doctoral dissertation, Univ. Calgary (Canada), 189p.
- Pavlidis, T., 1982. *Algorithms for Graphics and Image Processing*: Computer Science Press, Rockville, Maryland, 173p.
- PCI Inc., 1988. *EASI/PACE Image Analysis System Manual*: PCI Incorporated, Toronto, Ontario, Canada, variously paged.

- Peddle, D., and S. E. Franklin, 1991. Image texture processing and data integration for surface pattern discrimination: *Photogrammetric Engineering & Remote Sensing*, Vol. 57, No. 4, pp. 413-420.
- Qui, Z. C., and M. Goldberg, 1985. A new classification scheme based upon segmentation for remote sensing: *Canadian Jour. Remote Sensing*, Vol. 11, No. 1, pp. 59-69.
- Snyder, W. E., and A. Cowart, 1983. An interactive approach to region growing using associative memories: *IEEE Transactions on Pattern Analysis and Machine Intelligence*, Vol. 5, No. 3, pp. 349-352.
- Spann, M., and R. Wilson, 1985. A quadtree approach to image segmentation which combines statistical and spatial information: *Pattern Recognition*, Vol. 18, No. 3/4, pp. 257-269.
- Strahler, A., 1981. The use of prior probabilities in maximum likelihood classification of remotely sensed data: *Remote Sensing of Environment*, Vol. 10, No. 1, pp. 135-163.
- Swain, P. H., and S. M. Davis, 1978. *Remote Sensing, The Quantitative Approach*: McGraw-Hill, New York, 396p.
- Taylor, A., A. Cross, D. C. Hogg, and D. C. Mason, 1986. Knowledge-based interpretation of remotely sensed images: *Image and Vision Computing*, Vol. 4, No. 2, pp. 67-83.
- Tannous, I., and Arif, J. P. 1989. SAR images segmentation using region growing approach, *Proc. International Geoscience and Remote Sensing Symposium*, Vancouver, B.C., pp. 1209-1212.
- Thomas, I. L., 1980. Spatial postprocessing of spectrally classified Landsat data: *Photogrammetric Engineering & Remote Sensing*, Vol. 46, No. 9, pp. 1201-1206.
- Tilton, J. C., and S. C. Cox, 1983. Segmentation of remotely sensed data using parallel region growing, *Proc. Ninth Symposium on Machine Processing of Remotely Sensed Data*, LARS, Purdue Univ., West Lafayette, Indiana, pp. 130-137.
- Tom, C. H., and L. D. Miller, 1984. An automated land-use mapping comparison of the Bayesian maximum likelihood and linear discriminant analysis algorithms: *Photogrammetric Engineering & Remote Sensing*, Vol. 50, No. 2, pp. 193-207.

(Received 18 March 1991; accepted 29 April 1991; revised 14 June 1991)

Forum

The Case for the High Altitude Version of Landsat-7

THERE SEEMS TO BE GENERAL AGREEMENT (civilian and military) that Landsat should continue and that Landsat-7 should be designed as the first of a truly operational Earth sensing satellite of moderate resolution. There also seems to be agreement that Landsat-7 should preserve the best attributes of the existing civil systems but, in addition, provide a stereoscopic capability which will permit the development of a detailed topographic model of the Earth's land areas in a cost-effective manner.

The current major issues revolve around the basic parameters which will define Landsat-7; that is,

- Orbital altitude – 919 km versus 581 km
- Smallest pixel (GSD) – 10 m versus 5 m (resolution)
- Transmission data rate – 100 Mb/s versus 200 plus Mb/s

There are numerous other issues but, until these basic parameters (which are highly interrelated) are resolved, there is no way of defining the scope and cost of Landsat-7.

Basically, two conceptual designs are involved:

- High Altitude – to be flown at 919 km altitude with 10-m pixels and a data rate ≤ 100 MB/s as described in ITEK (1981) and by Colvocoresses (1991).
- Low Altitude – to be flown at 581 km altitude with 5-m pixels and a data rate ≥ 200 Mb/s as described by Light (1990).

The advantages of the 919-km orbit over the 581-km orbit for Earth sensing at a moderate resolution are

- Transmission coverage range is over 1.5 times greater, which means that the area covered by a single reception station is 2.5 times as great.
- Coverage swath width for systematic sequential coverage of a given sensor is determined by the orbital altitude (circular, sun-synchronous). For the 919-km orbit, this would be 180 km as compared to 64 km for the 581-km orbit. This means that a single scene (square) for the 919-km orbit would cover nearly 9 times the area as would a scene from the 581-km orbit. At highest (10-m) resolution and stereo coverage, swath width is reduced to 90 km in order to maintain the 100-Mb/s transmission rate.
- Frequency of coverage is an 18-day interval with the 919-km orbit and 45 days with the 581-km orbit. Thus, the 919-km orbit pro-

vides 2.5 times as many views of the same scene in any sizable time interval. The repeat frequency is halved from 18 days to 36 days at the highest stereo resolution.

- Orthogonality may be defined as the angle between the sensor path to the object and the local vertical. In the 919-km orbit case and using a vertically oriented sensor, this maximum angle off the vertical is 6.59x. The 581-km orbit case has similar orthogonal characteristics as long as the swath width is retained at 64 km but, if the swath is widened to increase coverage, the angle off the vertical rises accordingly. This creates many disadvantages from both the geometric and radiometric viewpoints.
- Continuity is maintained with respect to Landsats 1, 2, and 3 by using the 919-km orbit. Over ten years of Landsat MSS data were collected and archived from this orbit. Thus, those wishing to compare data of ten or more years separation can do so in a highly cost-effective manner even though the resolution and wave bands utilized for Landsat-7 may not be identical to those of the earlier Landsats.
- Orbital stability has been proven in the 919-km case. Although 581 km is well above atmospheric effects, the other conditions which create orbit anomalies (such as the Earth's ellipticity) are more pronounced at the lower orbit. Certainly, a longer life can be expected from a satellite at the higher orbit.
- Coverage patterns by which adjacent paths are covered on each successive day (east to west) are the same for both altitudes. However, very few other orbits of suitable height exist which provide such systematic coverage.

REFERENCES

- Colvocoresses, A. P., 1991. Landsat 7 – A Challenge to America, *Technical Papers, ACSM-ASPRS 1991 Annual Convention*, Vol. 3, 5 p.
- Light, Donald, 1990. Characteristics of Remote Sensors for Mapping and Earth Science Applications, *Photogrammetric Engineering & Remote Sensing*, Vol. 56, No. 12, pp. 1613-1625.
- ITEK, 1981. *Conceptual Design of an Automated Mapping Satellite System (MAPSAT)*, Final Technical Report, 285 p.

—Alden P. Colvocoresses
U. S. Geological Survey
Reston, VA 22092